

OPEN ACCESS

## Enhancement of Glucose Oxidase-Based Bioanode Performance by Comprising *Spirulina platensis* Microalgae Lysate

To cite this article: Rokas Žalnėravičius and Arunas Ramanavicius 2022 *J. Electrochem. Soc.* **169** 053510

View the [article online](#) for updates and enhancements.

### You may also like

- [Molybdenum-Dependent Formate Dehydrogenase for Formate Bioelectrocatalysis in a Formate/O<sub>2</sub> Enzymatic Fuel Cell](#)  
Selmihan Sahin, Rong Cai, Ross D. Milton et al.
- [Biofuel Cell Anodes Integrating NAD<sup>+</sup>-Dependent Enzymes and Multiwalled Carbon Nanotube Papers](#)  
Claudia W. Narváez Villarrubia, Sergio O. Garcia, Carolin Lau et al.
- [Platinum Nanoarrays Directly Grown onto a 3D-Carbon Felt Electrode as a Bifunctional Material for Garden Compost Microbial Fuel Cell](#)  
Widya Ernayati Kosimaningrum, Mekhaissia Ouis, Yaovi Holade et al.

**Investigate your battery materials under defined force!**  
The new PAT-Cell-Force, especially suitable for solid-state electrolytes!



- Battery test cell for force adjustment and measurement, 0 to 1500 Newton (0-5.9 MPa at 18mm electrode diameter)
- Additional monitoring of gas pressure and temperature

[www.el-cell.com](http://www.el-cell.com) +49 (0) 40 79012 737 [sales@el-cell.com](mailto:sales@el-cell.com)

**EL-CELL**<sup>®</sup>  
electrochemical test equipment





# Enhancement of Glucose Oxidase-Based Bioanode Performance by Comprising *Spirulina platensis* Microalgae Lysate

Rokas Žalnėravicius<sup>1</sup>  and Arunas Ramanavicius<sup>1,2,z</sup> 

<sup>1</sup>Centre for Physical Sciences and Technology, LT-10257 Vilnius, Lithuania

<sup>2</sup>Vilnius University, Faculty of Chemistry and Geosciences, Institute of Chemistry, Department of Physical Chemistry, LT-03225, Vilnius, Lithuania

In this study, *Spirulina platensis*-based lysate was used as a biological redox mediator to design glucose oxidase (GOx) based biofuel cell bioanode. Chemically oxidized multi-walled carbon nanotubes (CNT) were deposited on carbon-electrode and were covered with eco-friendly algae cell-based lysate that facilitated the electron transfer and served as a biocompatible matrix for enzyme immobilization, which reduced the inactivation of GOx by CNT. The designed GC/PEI/CNT/S.p./GOx bioanode exhibited an open circuit potential (OCP) of  $-262$  mV vs Ag/AgCl<sub>(3M KCl)</sub> in the presence of 12.5 mM of glucose. The maximum power output of the proposed bioanode was 21.8 times higher and reached  $3.2 \mu\text{W cm}^{-2}$  at  $-51$  mV vs Ag/AgCl<sub>(3M KCl)</sub> if the *S. platensis* cell lysate was used for bioanode design. The amperometric responses of GC/PEI/CNT/S.p./GOx bioelectrode towards the addition of glucose were linear at glucose concentrations ranging between 250  $\mu\text{M}$  and 5 mM. These characteristics enable applying this bioanode as a part of biofuel cell and the electrode of an amperometric glucose biosensor, which response within 15 s, with a detection limit of 118  $\mu\text{M}$  and a sensitivity of  $15.09 \mu\text{A mM}^{-1} \text{cm}^{-2}$ .

© 2022 The Author(s). Published on behalf of The Electrochemical Society by IOP Publishing Limited. This is an open access article distributed under the terms of the Creative Commons Attribution 4.0 License (CC BY, <http://creativecommons.org/licenses/by/4.0/>), which permits unrestricted reuse of the work in any medium, provided the original work is properly cited. [DOI: 10.1149/1945-7111/ac7080]



Manuscript submitted March 23, 2022; revised manuscript received May 4, 2022. Published May 27, 2022.

According to the report launched by United Nations, it was estimated that the global population growth will increase, expecting to achieve over 9.7 billion people in 2050 and 10.9 billion people in 2100.<sup>1</sup> By comparing with today's numbers, the population of humans will increase almost 25% by 2050, thus predicting an increase in the entire world's energy consumption by over 50%.<sup>2</sup> Taking into account that today, almost 80% of all energy demand is generated from non-renewable sources such as gas, oil, coal, which utilization mainly affects the Earth's climate change, the development of alternative "green" technologies is one of the most significant challenges facing the research community.<sup>3</sup> Bioelectrochemical systems (BES), including enzymatic and various microorganisms-based biofuel cells, can encourage alternative techniques for generating renewable energy or valuable products such as hydrogen, methane, peroxides or heavy metals.<sup>4</sup> These biological systems can be employed for organic pollutants containing wastewater purification and simultaneously produce bioelectricity by utilising organic matter at the anode chamber designed with electroactive bacteria films or active redox enzymes.<sup>5</sup> However, some limitations are mostly related to their low efficiency and long-term stability to be overcome to apply these technologies to commercial applications.<sup>6</sup> The higher efficiency of biofuel cells can be realized if the biological catalysts are capable of undergoing direct electron transfer (DET) between themselves and electrode material,<sup>7</sup> on which it has to be immobilized.

The ability to undergo DET depends on the enzyme's crystal structure, the cofactor's nature, and its localization in the enzyme matrix. According to Gray et al. investigations, the distance between cofactor and enzyme surface plays a significant role in its DET efficiency, caused by the electron tunnelling effects.<sup>8</sup> Regarding Dutton's group observations, the electron transfer effectiveness through the proteins decreases exponentially by increasing the distance between the redox centre of the enzyme and the electrode. This distance extremely increases when the redox centre is deeply buried within the protein matrix of the enzyme. It was concluded that for a rather rapid electron transfer, this distance needs to be lower than  $\sim 8$  Å, while a further increase between 8 and 17 Å leads to the reduction of DET efficiency over 10,000 times.<sup>9</sup> In some cases, this distance requirement is limited by the enzyme's nature, similarly to glucose oxidase (GOx) from *Aspergillus niger*, whereas its cofactor

of flavin adenine dinucleotide (FAD) is deeply buried into the enzyme matrix by at least 17 Å.<sup>10</sup> Despite this fact, GOx is the most frequently used enzyme in developing biosensors and biofuel cells due to its good stability and high catalytic activity.<sup>11</sup> From this perspective, the DET of GOx on various carbon-containing nanomaterials is often claimed in the literature. Nevertheless, the most likely observed evidence is the FAD redox pair at  $-0.45$  V vs Ag/AgCl (pH = 7) and the cathodic current decrease upon glucose addition. Recently, Bartlett et al. proved that there is no valid evidence for DET provided by GOx.<sup>10</sup> Wilson earlier highlighted a similar statement, clearly explaining that the DET of GOx was inaccurately interpreted in the vast majority of scientific papers due to the unappreciated interference of free FAD adsorbed on CNT.<sup>12</sup> Therefore, regarding these studies, the claim of DET for any enzymatic process should be carefully evaluated and justified by a series of additional experiments.

The development of nanotechnology leads to accomplishing the larger surface via involving various nanomaterials such as gold, silver, carbon-based materials, including carbon nanotubes (CNT), fullerene, graphene oxide, etc. or quantum dots in the electrode design, thus ensuring the superior communication between biological catalysts and electrode.<sup>13,14</sup> Recently, the *Spirulina platensis* microalgae, commonly known because of their biomass enriched with proteins, vitamins and antioxidants and are already commercialized as a food supplement,<sup>15</sup> have been used to prepare algae-based biofuel cells. These cyanobacteria do not need any expensive nutrients for their cultivation. They can be grown even on wastewater using CO<sub>2</sub> from the air and the Sunlight required to carry out the photosynthesis,<sup>16</sup> thus making these algae cells more advantageous for sustainable "green" energy production. Lin et al. have shown that *S. platensis* formed biofilm provides the maximal open circuit potential (OCP) value of 0.49 V. This photosynthetic biofuel cell exhibited the maximum power output of  $10 \text{ mW m}^{-2}$  registered at the external resistance of 1 kΩ.<sup>17</sup> More recently, Longtin et al. discovered the long-life bioanode comprised of algae living cells, which generate the power density of  $59.8 \text{ mW cm}^{-2}$  and the OCP magnitude of 227.7 mV calculated on the 7th day measurements.<sup>18</sup> Yang et al. designed the algae biofilm microbial fuel cell (ABMFC) that provides a higher power density of  $62.93 \text{ mW m}^{-2}$ .<sup>19</sup> However, to the best of our knowledge, the algae cell lysate has never been used for organelle-based biofuel cells design; thus, the relationship between *S. platensis*-based lysate and GOx enzyme on carbon-

<sup>z</sup>E-mail: Arunas.Ramanavicius@chf.vu

modified electrodes remains unclear, which should be further justified.

In the present study, the *S. platensis*-based lysate was used as a cheap and green alternative for mediators such as flavins, phenazines, and quinones that shuttle the electrons from the redox centre to the solid electrode. Instead of these expensive compounds, the *S. platensis*-based lysate serves as a biological redox mediator for the GOx enzyme, reducing the OCP drop along the electron pathways and facilitating the electron transfer between the redox-active centre and CNT modified electrode. The designed bioanode marked as GC/PEI/CNT/S.p./GOx exhibits a 21.8 times higher power output ( $3.2 \mu\text{W cm}^{-2}$ ), determined at the potential of  $-51 \text{ mV vs Ag/AgCl}$  (3 M KCl). The series control experiments with guanidine hydrochloride, dialysis membrane, L-glucose, ferrocene and others show that the origin of cathodic current reduces upon the addition of glucose observed via CV and chronoamperometry methods are mainly attributed not to DET as usually claimed in literature but to the depletion of oxygen in the buffer solutions. Based on these results, it was demonstrated that this phenomenon could also be applied to develop glucose biosensors. The amperometric responses of GC/PEI/CNT/S.p./GOx bioelectrode towards the addition of glucose were linearly at glucose concentrations ranging between  $250 \mu\text{M}$  and  $5 \text{ mM}$ . The electrode exhibited a response time of  $14.5 \text{ s}$ , detection limit of  $118 \mu\text{M}$  and sensitivity of  $15.09 \mu\text{A mM}^{-1} \text{ cm}^{-2}$ .

### Experimental

**Materials and reagents.**—All reagents in this study were of analytical grade and were used as obtained without further purification unless otherwise specified. Glucose oxidase (E.C.1.1.3.4., GOx) from *Aspergillus niger* (specific activity  $\sim 295 \text{ U mg}^{-1}$ ), catalase (E.C.1.11.1.6.) liquid solution from bovine liver (enzymatic activity  $132,000 \text{ CIU ml}^{-1}$ ), multi-walled carbon nanotubes (CNT, diameter ranges from 6 to 13 nm, 98% carbon basis), glutaraldehyde (25% wt. in water), polyethyleneimine (PEI, branched,  $M_w \sim 25,000$ , 99%), guanidine hydrochloride (98%), ferrocene (98%), L-glucose (99%), hydrogen peroxide (34.5%–36.5%), sulfuric acid (95%–97%) and trisodium citrate (99%) were purchased by Sigma-Aldrich Chemical Co. All salts used for preparations of phosphate/acetate buffer solutions (signed as A-PBS) with the composition of  $47 \text{ mM}$  potassium dihydrogen phosphate,  $3 \text{ mM}$  dipotassium hydrogen phosphate,  $50 \text{ mM}$  sodium acetate and  $100 \text{ mM}$  potassium chloride

( $\text{pH} = 6$ ) were received from Reachem Slovakia S.r.o. The potassium chloride (99%), potassium dihydrogen phosphate (99%), dipotassium hydrogen phosphate (99%) and sodium acetate (99%). D, L-glucose (99%) was obtained from Alfa Aesar. The  $12 \text{ kDa}$  dialysis membrane used for GC/PEI/CNT electrode isolation was purchased from Thermo Scientific (USA). The glassy carbon electrodes (GC, Sigradur G) with a geometric surface area equal to  $0.07065 \text{ cm}^2$  were obtained from HTW (Germany) and used as a basic material for bioelectrode design. Prior to using the GC electrodes for bioelectrode design, their surfaces were mechanically polished with  $0.3$ , and  $1 \mu\text{m}$  sized  $\text{Al}_2\text{O}_3$  paste received from BASi (USA). The new  $1 \text{ mol l}^{-1}$  of glucose solution was prepared at least  $24 \text{ h}$  before measurements. *Spirulina* (*Arthrospira*) *platensis* (NIVA-CYA 428) algae cells were purchased from NORCCA (Norway). All buffer and rinsing solutions used for cleaning the bioelectrodes and washing the CNT powders were prepared using deionized Milli-Q water ( $18 \text{ M}\Omega\cdot\text{cm}$ ).

**Microalgae-based lysate preparation.**—As-received cells were washed several times with a physiological solution of  $0.9\%$  NaCl, then collected by centrifugation at  $300 \text{ G}$  for  $10 \text{ min}$ . Next, the cell lysis was completed using a probe sonicator (Sonics, UK) under the sonication frequency of  $20 \text{ kHz}$  (with an amplitude of  $15\%$ ) and the power regime of  $130 \text{ W}$ . Prior to the cell lysis, the green precipitate was suspended in A-PBS solutions and transferred into the ice-surrounded plastic tube which protects the samples from over-heating. Then, samples were subjected to sonication for  $30 \text{ min}$ . Finally, the cell debris was removed from the solution via centrifugation at  $\sim 540 \text{ G}$  for  $10 \text{ min}$ . The obtained lightly green in the colour protein-enriched lysate was further analysed using a protocol proposed by Bradford et al.<sup>20</sup> and applied for bioelectrode constructions.

**GOx-based bioanode construction procedures.**—Firstly, the GC electrodes were mechanically cleaned using fine-grit polishing pads (BASi) wetted with different-sized  $\text{Al}_2\text{O}_3$  paste. Afterwards, the electrodes were thoroughly rinsed with DI water and consecutively cleaned via potential cycling. Next, the refined electrodes were immersed in the new aqueous PEI ( $1 \text{ mg ml}^{-1}$ ) solution for  $5 \text{ min}$  to provide a positive charge on the GC surface and carefully rinsed with DI water. It should be noted that multi-walled carbon nanotubes used to construct bioelectrodes were firstly chemically oxidized in a

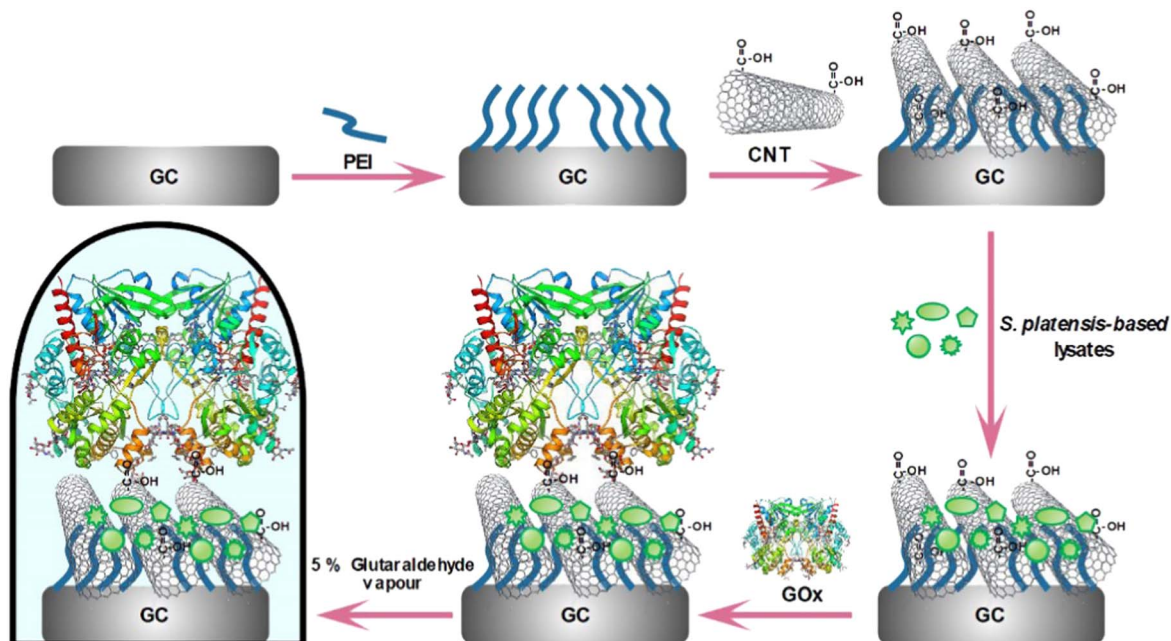


**Figure 1.** The principle design scheme of GC/PEI/CNT/S.p./GOx bioanode based on microalgae cell lysate utilization as biological redox mediator.

concentrated acidic solution of  $\text{H}_2\text{SO}_4:\text{HNO}_3$  with a ratio of 3:1 (v/v) at  $40^\circ\text{C}$  for 8 h. This modification leads to the oxygen-containing group's formation on the CNT surface,<sup>21</sup> thus enhancing their wetting properties and ensuring their better dispersion degree in polar solutions.<sup>22</sup> Prior to use, the chemically oxidized CNT were subjected to sonication for 24 h, and  $5\ \mu\text{l}$  of a black solution containing  $5\ \text{mg}\ \text{ml}^{-1}$  of functionalized CNT were drop-casted on GC electrodes. Then, the GC/PEI/CNT electrode composition was further enriched with *S. platensis*-based lysate, used in this research as a biocompatible and biological molecule conjugate that can facilitate immobilization of enzyme and probably can act as an electron carrier. Following this approach, the  $5\ \mu\text{l}$  of algae lysate was dropped on the electrode surface and left to dry under ambient conditions to achieve this purpose. The main construction steps of bioanode are highlighted in the schematic illustration presented in Fig. 1. lastly, the  $5\ \mu\text{l}$  of GOx solution ( $10\ \text{mg}\ \text{ml}^{-1}$ ) was placed on the top of the electrode and enclosed with the Eppendorf cups partially filled with 5% of glutaraldehyde. Then, the prepared bioanode was transferred into the fridge and kept for 16 h under the glutaraldehyde vapour at  $4^\circ\text{C}$ , which was utilized to cross-link the enzymes as described in detail previously.<sup>23</sup>

Notably, the constructed bioanode (denoted as GC/PEI/MWCNT/S.p./GOx) was soaked into an A-PBS buffer and stored in the fridge if not in use. In order to evidence the presence of free FAD in the solution of GOx, the GC/PEI/CNT electrode was gently covered with a 12 kDa dialysis membrane, which was soaked in DI water overnight and fixed by silicone-based O-rings. The control measurements were conducted herein to clarify the possible influence of the catalase enzyme, known as a "residual impurity" of commercially available GOx<sup>24</sup> for cyclic voltammetry results interpretation. For this objective, the bioanode design (marked as GC/PEI/MWCNT/S.p./CAT) was prepared in the same way except for the final step, whereas  $5\ \mu\text{l}$  of catalase was used instead of GOx enzyme.

**Electrochemical measurements.**—Using Zahner Zennium electrochemical workstation (Zahner-Elektrik, Germany), electrochemical measurements were carried out using three-electrode configuration cells. The GC/PEI/CNT/S.p./GOx bioanode was operated as a working electrode. The Ag/AgCl was filled with 3 M KCl ( $+205\ \text{mV}$  vs SHE), and the platinum sheet with the dimensions of  $12 \times 35\ \text{mm}$  was employed as a reference and auxiliary electrodes, respectively. All experimental potentials given in this study are relative to the Ag/AgCl (3 M KCl) unless otherwise specified. The influence of oxygen, hydrogen peroxide and possible metal oxide-based impurities ( $\text{MeO}_x$ ) that are incorporated into CNT structure on the catalytic properties of GC/PEI/CNT/S.p./GOx bioanode were evaluated via cyclic voltammetry (CV) at the

potential window ranging from  $-1000$  to  $600\ \text{mV}$  and the potential scan rate of  $40\ \text{mV}\ \text{s}^{-1}$ . In order to determine the CNT catalytic properties and possible interferences with the catalytic current produced by GC/PEI/CNT/S.p./GOx bioanode, the CV scan was registered under similar conditions A-PBS buffer solution ( $\text{pH} = 6$ ) containing  $12.5\ \text{mM}$  of glucose. The open-circuit potential (OCP) of proposed bioelectrodes was established by running the chronoamperometry measurements in the two-electrode electrochemical cell with the negligible current ( $\sim 1\ \text{pA}$ ) flowing through the system.

Similarly, the polarization and power density measurements were carried out by sweeping the potential directly from OCP to zero at the scan rate of  $0.1\ \text{mV}\ \text{s}^{-1}$  using the linear sweep voltammetry (LSV) method in a single-compartment electrochemical cell by connecting the GC/PEI/CNT/S.p./GOx bioanode as the working electrode and the glassy carbon cathode with the surface area of  $2.0\ \text{cm}^2$  as a combined reference and counter electrode.<sup>25</sup> The relative stability of GC/PEI/CNT/S.p./GOx bioanode was examined each day over seven days in the presence of  $12.5\ \text{mM}$  of glucose. The amperometric responses were evaluated for different glucose injections under the magnetic stirring of air-saturated A-BPS solution at an applied voltage of  $-0.18$  and  $+0.15\ \text{V}$  vs Ag/AgCl (3 M KCl). To clarify the origin of four well-defined redox peaks registered during CV scans and their "catalytic" response towards the addition of glucose, several control experiments were conducted in air-saturated and oxygen-free (saturated by purging with  $\text{N}_2$  gas for 2 h) A-PBS solution using L-glucose, guanidine hydrochloride, dialysis membrane, catalase and ferrocene as a redox mediator.

## Results

**Electrochemical activity of CNT and their metal oxide-based impurities.**—Frequently, CNT employment in biosensors and biofuel cells is related to their unique properties such as high specific surface, excellent electrical conductivity, nanowire morphology, and capability to reach the prosthetic group of the enzyme.<sup>26</sup> DET promotion between enzyme redox centre to the bulk electrode is highlighted in many scientific papers.<sup>27,28</sup> However, we should note that claiming the mediator-less DET of GOx on CNT is still questionable due to complex heterogeneous reactions that occur on the CNT-modified bioelectrode. Notably, the CNT used as a substrate for biomolecules immobilization was modified by oxygen-containing groups via an acidic oxidation process. Firstly, the influence of CNT and some metal oxide-based impurities in their composition even after acidic or alkaline purification on the enzymatic electrode performances were investigated herein. It is known that oxygen reduction (ORR), as well as hydrogen peroxide ( $\text{H}_2\text{O}_2$ ) reduction reactions, are susceptible to metal oxide-based impurities.<sup>10</sup> These reactions become less efficient if the CNT

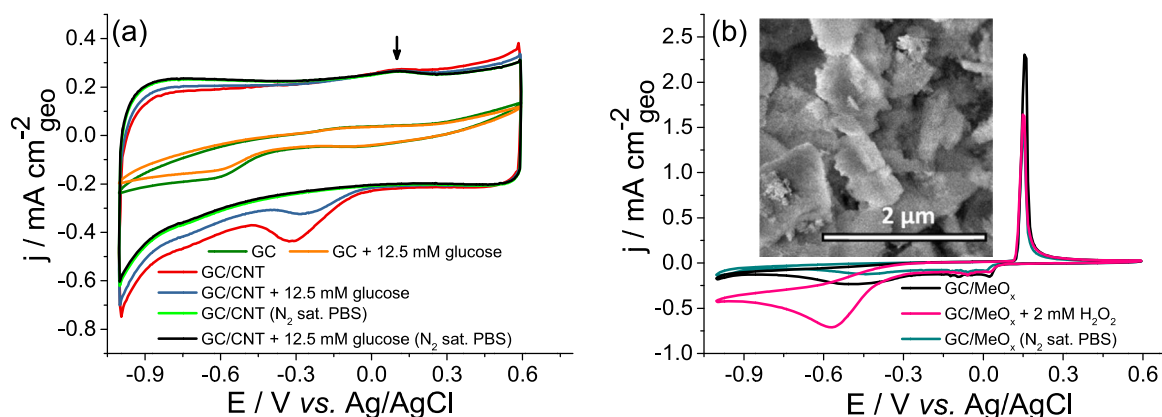


**Figure 2.** Cyclic voltammograms of different electrode designs were recorded in air and  $\text{N}_2$  saturated A-PBS ( $\text{pH} = 6$ ) without and in the presence of  $12.5\ \text{mM}$  of glucose at the potential window of  $1.0$  to  $-0.6\ \text{V}$ , a scan rate of  $40\ \text{mV}\ \text{s}^{-1}$ . Cyclic voltammograms of bare GC, GC/CNT electrode (a) and GC decorated with  $\text{MeO}_x$  traces (b) were registered after the combustion of CNTs in the air at  $700^\circ\text{C}$  for 4 h in the presence of  $2\ \text{mM}$  of  $\text{H}_2\text{O}_2$ . Insets: top-side SEM image of the  $\text{MeO}_x$ -based products obtained after the oxidation of CNTs.

surface is covered with some organic molecules such as enzymes, various cell organelles, and probably cell lysate due to the occupation of their active sites. However, it can affect the catalytic current generated by bioelectrode, especially at the negative potential ranges in oxygen-enriched buffer solutions. In order to clarify these reactions more in detail, the cyclic voltammetry was performed at the potential window of  $-1000$  to  $600$  mV with different GC electrode designs in  $N_2$  and air-saturated A-PBS at a scan rate of  $40$  mV  $s^{-1}$  (Fig. 2a). From cyclic voltammograms (Fig. 2a), it is seen that onset potential (potential values at which the reaction starts) of ORR on GC and GC/CNT take place at  $-350$  and  $78$  mV, respectively. The oxygen reduction on CNT has a prominent reduction peak with an  $E_{pc}$  value of  $-319.9$  mV. However, after removing dissolved oxygen by bubbling the  $N_2$  gas for two hours, the reduction peak disappeared, following the decrease in cathodic current density, confirming its origin in the ORR. It should be noted that after the addition of  $2$  mM  $H_2O_2$ , no significant changes in current were observed, and the CV profile remains identical to that registered in the case with GC/CNT (Fig. 2a). However, in the presence of  $12.5$  mM glucose, the reduction current started to decrease from  $-255$  mV and  $65$  mV in a case with GC and GC/CNT electrodes, respectively (Fig. 2a).

This decrease probably is a consequence of glucose adsorption on the active CNT surface, thus reducing the active area of CNT suitable for ORR on which it appears at more positive potential due to metal oxide-based impurities that are promising catalysts for ORR.<sup>29</sup> On the other hand, it can be related to the increase in solution viscosity, causing the slower  $O_2$  molecules diffusion. On the contrary, the addition of  $12.5$  mM glucose does not cause any significant changes in the current profile when measuring in  $O_2$ -free buffer solutions, as evidenced by curves presented in Fig. 2a and supports the explanations described above. Therefore, these reactions need to be considered to evaluate the performance of the bioelectrode that was designed by utilizing the CNT layer.

More exciting results were determined from CV measurements with GC/MeO<sub>x</sub> electrode design. To examine the influence of metal oxides-based impurities that exist in commercial CNT structure on the bioelectrode performances, the CNT was combusted under the synthetic air atmosphere at  $1000$  °C for 2 h. This procedure reduces the carbon content, increasing the ratio of metal oxides-based impurities and ensuring higher electrochemical relevance. The obtained powder, marked as MeO<sub>x</sub>, was placed on the GC electrode and analysed via cyclic voltammetry. The sharp oxidation peak with an  $E_{pa}$  value of  $153$  mV observed herein is related to the oxidation of metal oxide-based impurities (Fig. 2b). This peak is also visible in a GC/CNT electrode (Fig. 2a, black arrow). The reduction curve profile has one negligible and visible cathodic current increase region with starting potentials of  $57$  and  $-173$  mV, respectively. The first can be attributed to MeO<sub>x</sub> reduction or ORR occurring at a higher potential on these metal oxides such as Co, Al, and V-based surfaces.<sup>30</sup> ORR mainly induces the second one because the current decrease is more effective after oxygen removal. In the presence of  $2$  mM of  $H_2O_2$ , the cathodic current started to decrease due to peroxide reduction on MeO<sub>x</sub> surface with an onset potential of  $-148$  mV, the  $E_{pc}$  value of  $-572$  mV and the  $\Delta j_{pc}$  of  $-0.61$  mA  $cm^{-2}$ . The sensitivity of GC/MeO<sub>x</sub> electrode towards  $H_2O_2$  reduction estimated from CV was determined to be  $0.25$   $\mu A$   $\mu M^{-1}$   $cm^{-2}$  proving that the metal oxides released by CNT combustion are promising electrocatalysts and can be used for the preparation of non-enzymatic  $H_2O_2$  sensors.

#### Electrochemical activity of GC/PEI/CNT/S.p./GOx bioanode.—

The origin of four well-defined redox peaks recorded via cyclic voltammetry (Fig. 3a, marked with arrows) have been related to FAD/FADH<sub>2</sub> and unknown electroactive species of microalgae cell lysate. By reviewing past literature, the cathodic current decrease in the presence of glucose is usually claimed as true evidence of direct electron transfer (DET) between various nanomaterials and the GOx enzyme's redox centre. However, recent studies with a more precise

explanation of this phenomenon have been proposed, showing that this effect can be attributed to oxygen depletion.<sup>10,12</sup> To prove this assumption, the influence of oxygen, CNT, hydrogen peroxide, glucose or even free FAD and catalase, that known to be impurities of available commercial GOx and can quickly adsorb on the CNT surface,<sup>31</sup> needs to be considered when interpreting the performances of GOx-based bioelectrodes. All summarized processes occur mainly in the cathodic region; thus, the cathodic potential region was investigated by cyclic voltammetry to ensure more precise information. The presence of  $12.5$  mM of glucose resulted in a decrease in cathodic current (Fig. 3a), mainly caused by a dramatically reduced ORR rate due to oxygen depletion in the solution. These results were further evidenced by recording the CV's scan in the oxygen-free solutions, whereas the cyclic voltammogram exhibits an identical profile even after  $12.5$  mM of glucose (Fig. 3a). It should be noted that the impact of ORR that occurs on the CNT surface can be eliminated by removing the dissolved oxygen in the electrolyte, as evidenced by the  $O_2$  reduction peak disappearance shown in Fig. 2a. Besides that, this peak appears in  $O_2$  containing solutions at a lower potential range with an  $E_{pc}$  value of  $-315$  mV. (Fig. 3a, marked with arrow) and do not interfere with the biologically relevant redox peaks observed herein. Surprisingly, a similar phenomenon was observed in a case with an enzyme-less GC/CNT electrode design, which was related to the current decrease after the addition of glucose (Fig. 2a). This observation probably arises from the adsorption of glucose on CNT, thus blocking their active sites suitable for ORR or changes in solution viscosity, affecting the oxygen diffusion. Furthermore, it was hypothesized that a small fraction of this cathodic current might be related to  $H_2O_2$  (produced by enzymatic reaction or ORR<sup>32</sup>) reduction on the metal oxide-based impurities, as illustrated above. However, after adding  $2$  mM  $H_2O_2$ , the CV profile remains similar to GC/PEI/CNT/S.p./GOx (data not shown), thus clarifying the quantity of metal oxides in CNT is negligible toward  $H_2O_2$  reduction. Furthermore, it is also known that catalase (CAT) is one of the most likely impurities that uses  $H_2O_2$  as a substrate and can be found in commercial GOx, with the ratio between GOx and CAT depending on the supplier's, varying from  $7.5$  to  $30$ .<sup>10</sup>

From this perspective, the interference of CAT to GOx-based bioelectrode performances should be less significant. However, it can influence the registered catalytic current via hydrogen peroxide (produced via enzymatic reaction) conversion to oxygen and water catalysed by CAT enzymes. As shown in Fig. 3b, this process occurs at the potential region close to the FAD/FADH<sub>2</sub> redox potential with an  $E_{pc}$  value of  $-312$  mV (vs Ag/AgCl); thus, in some cases, it might interfere with the "catalytic" current assessments. However, as noted above, the addition of hydrogen peroxide does not cause any visible changes for GC/PEI/CNT/S.p./GOx electrode in the CV profile, thus ensuring that the presence of catalase is too low in GOx (type VII, Sigma Aldrich) powder. Finally, it can be summarized that this factor can be ignored only at the potential window tested herein when characterizing the CNT-based biosensors and biofuel cells.

In order to characterize these two quasi-reversible redox pair CV-peaks more in detail, the heterogeneous electron transfer rate constants ( $K_s$ ) were estimated using Laviron's equation.<sup>33</sup> The dependencies of  $E_{pa}$  and  $E_{pc}$  on the logarithm scan rate (Figs. 3c and 3d) can be linearly fitted at scan rates usually higher than  $200$  mV  $s^{-1}$ , thus giving the slope which is directly proportional to  $2.3RT/(1-\alpha)nF$  and  $-2.3RT/\alpha nF$ , corresponding to the anodic and cathodic peaks, used for calculation of the charge transfer coefficient ( $\alpha$ ). In this study, the transfer coefficients were found to be  $0.68$  and  $0.7$ , whereas the  $K_s$  constant is equal to  $17.3$  and  $7.6$   $s^{-1}$  for GOx and *S. platensis* based redox species. Considering the fact that both processes are surface-controlled, as evidenced above, the estimated  $K_s$  value for FAD/FADH<sub>2</sub> is higher than those reported in the previous studies, whereas the  $K_s$  ranged from  $\sim 2$  to  $12$   $s^{-1}$ .<sup>34</sup> This distinction was possible observed due to *S. platensis* lysate usage, which might be served for enzyme immobilization via reducing the

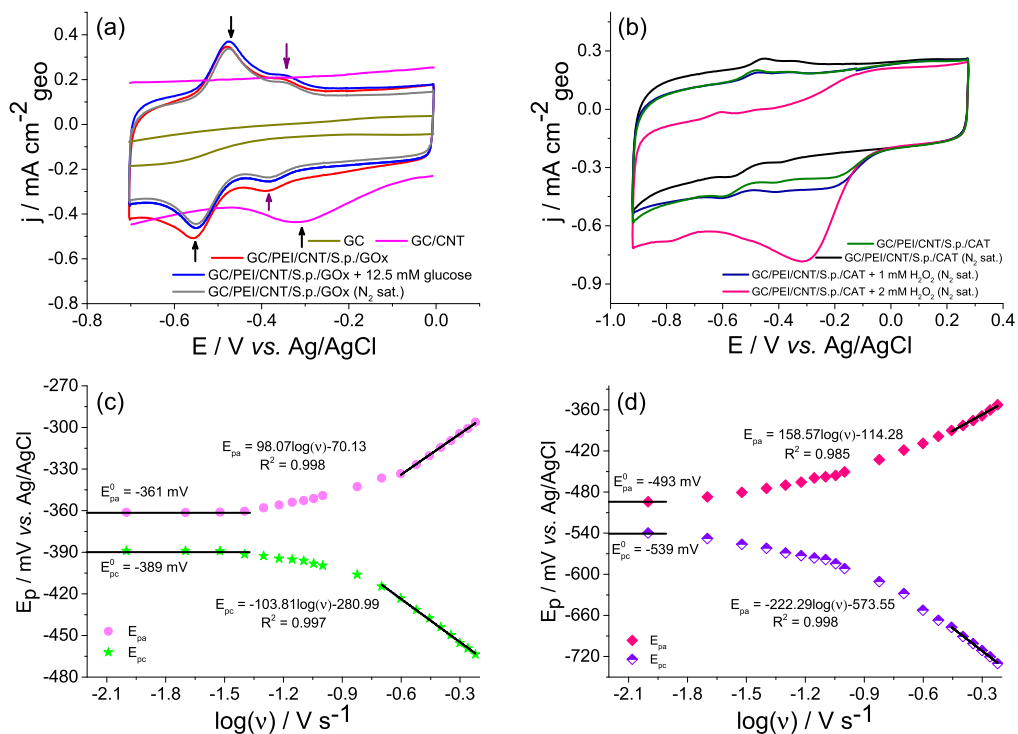


**Figure 3.** Cyclic voltammograms of GC/PEI/CNT/S.p./GOx (a) and GC/PEI/CNT/S.p./CAT (b) electrodes recorded in N<sub>2</sub> and air-saturated A-PBS solution (pH = 6) in the presence and the absence of 12.5 mM of glucose and 1 or 2 mM of hydrogen peroxide at a constant scan rate of 40 mV s<sup>-1</sup>. Laviron's plots of FAD/FADH<sub>2</sub> (c) and *S. platensis* lysate (d) peak potential  $E_{p(a,c)}$  as a function of the logarithm of scan rate recorded in N<sub>2</sub>-saturated A-PBS.

“side” effects of CNT to enzyme conformation and possible facilitating the electron transfer. On the other hand, this difference could be related to the free FAD redox couple, which is adsorbed on CNTs covered by *S. platensis* lysate, which possesses an extremely high electron transfer rate.

The registered redox waves of unknown redox-active species raised due to *S. platensis*-based lysate utilization in bioanode design indicate that it cannot be assigned as a redox mediator because of its more reductive formal potential equal to  $-521.5 \text{ mV}$  (vs Ag/AgCl). However, according to the chronoamperometric results (data not shown), the addition of glucose at the constant potential of  $+150 \text{ mV}$  (vs Ag/AgCl) leads to the increase of current provided by GC/PEI/CNT/S.p./GOx bioanode with  $I_{\text{max}}$  equal to  $20 \mu\text{A cm}^{-2}$ . This dependence disappeared if the *S. platensis*-based lysate was not comprised in the bioelectrode design. This phenomenon can be clarified as follows: the *S. platensis* lysate consists of only a small fraction of redox species that are invincible by recording the CV but still can act as a redox mediator for GOx either the *S. platensis* lysate facilitate GOx immobilization on the electrode and probably serve as the electron carrier. In order to prove this assumption, the GOx coverage efficiency was investigated by using the UV-vis spectrophotometry method by analysing the GOx residual in the solution after enzyme immobilization. For this purpose, the higher GC electrode ( $S = 1 \text{ cm}^2$ ) was chosen herein to ensure better accuracy and was prepared following the same procedures as shown in Fig. 1. After enzyme immobilization, the GC, GC/PEI/CNT/GOx and GC/PEI/CNT/S.p./GOx electrodes were separately washed with A-PBS, and the absorbance spectra were registered and compared to the calibration curve (data not shown). All absorption spectra have the maximum absorption peak at 266 nm, assigned as the polypeptide chains of native GOx in the buffer solutions.<sup>35</sup> It was observed that the bare GC surface is unsuitable for GOx immobilization, whereas the surface coverage reached only  $9.38 \text{ pmol cm}^{-2}$ . A higher value of surface loading equal to  $133.4 \text{ pmol cm}^{-2}$  was obtained with CNT modified GC electrode. This effect can be assigned to its high specific surface area. Surprisingly, the highest surface coverage of  $154.6 \text{ pmol cm}^{-2}$  was obtained when the *S. platensis* based lysate

was used for bioelectrode design. These results match those obtained with ferrocene redox mediator (presented below), whereas the registered catalytic current was 10.4% higher if algae lysate was composed of bioanode design, proving their essential role in the case of GOx immobilization.

**Microalgae-based bioanode characteristics.**—The microalgae cell's utilization in the development of biofuel cells has received considerable attention from the research community due to its ability to be adapted to various applications, including food supplements, vitamin production or “green” electricity generation.<sup>18,36</sup> Besides that, the growing conditions required to cultivate *S. platensis* cyanobacteria are relatively simple and cheap, making it more advantageous.<sup>37</sup> However, its lysate has never been used to prepare biosensors and biofuel cells. In this study, the *S. platensis*-based lysate was investigated as a suitable biological molecule conjugate that facilitates the GOx enzyme immobilization and improves the electron transfer rate. The influence of microalgae cell lysate on GC/PEI/CNT/S.p./GOx bioelectrode performance was assessed by estimating the open circuit potential (OCP) and power density measurements. Before power measurements, the OCP of bioanode and cathode were measured separately using the Ag/AgCl (3 M KCl) reference electrode in a single-compartment cell. It was found that the initial OCP value was  $-156 \text{ mV}$  (vs Ag/AgCl) if the microalgae lysate was incorporated into the bioelectrode design. Furthermore, in the presence of 12.5 mM of glucose, this value dropped to  $-262 \text{ mV}$  (vs Ag/AgCl), indicating that *S. platensis*-based lysate enhances the electron transfer rate and reduces the overpotential of glucose oxidation.

This relatively high negative potential plays an essential role for GC/PEI/CNT/S.p./GOx bioelectrode to act as a bioanode in a one-compartment biofuel cell design. The potential difference between a reference electrode and a bare glassy carbon cathode was  $+95 \text{ mV}$  (vs Ag/AgCl). The obtained potential difference determined the maximal whole-cell OCP of the biofuel cell and was  $357 \text{ mV}$  for the bio device operating in an A-PBS buffer containing 12.5 mM of glucose. Power output was determined using the linear sweep

voltammetry (LSV) method and two-electrode cell configuration. The registered power and current density of GC/PEI/CNT/S.p./GOx electrode were approximately 21.8 and 10.7 times higher than GC/PEI/CNT/GOx, respectively (Figs. 4a and 4b). It was determined that GC/PEI/CNT/S.p./GOx bioanode generated 357 mV potential (the highest OCP value reached 12.5 mM of glucose) at the load of 0.54 M $\Omega$  (Fig. 4c). Furthermore, the maximum power density of GOx-based bioanode was found to be 0.146  $\mu\text{W cm}^{-2}$ , thus supporting the idea that GOx does not undergo DET without any additional services of redox-active species. In contrast, if biological *S. platensis*-based lysate was used in the bioelectrode design, this value increased over 21.8 times and reached 3.2  $\mu\text{W cm}^{-2}$ . Furthermore, the stability assessments have shown that GC/PEI/CNT/S.p./GOx bioanode exhibits long-term stability over seven days, losing only 10.4% of its maximal averaged power efficiency (data not shown). These results confirm the hypothesis that biological and eco-friendly *S. platensis*-based lysate can facilitate enzyme immobilization, probably by preventing the possible CNT “side” effects and enhancing the electron transfer rate suitable for the construction of biosensors and biofuel cells.

**Electrocatalytic activity of GC/PEI/CNT/S.p./GOx bioelectrode.**—In order to further investigate the electrocatalytic properties of GC/PEI/CNT/S.p./GOx bioelectrode towards different glucose concentrations, the chronoamperometric measurements were conducted in the air-saturated A-PBS solution under the constant potential of  $-385$  mV. From a typical  $i-t$  curve presented in Fig. 6a, it is obvious that after continuous injection of 1 mM glucose, the current response of GC/PEI/CNT/S.p./GOx bioelectrode decreased, showing hyperbolic dependence and reached the steady-state condition when the substrate concentration exceeds 3 mM (Fig. 5b). The magnitude of the current response decreased linearly following the equation of  $J$  ( $\mu\text{A cm}^{-2}$ ) =  $-7.91 \cdot 10^{-6} \cdot C$  (mM) +  $2.69 \cdot 10^{-5}$  ( $R^2 = 0.958$ ) at the glucose concentration ranging between 1 and 3 mM. The registered response time of GC/PEI/CNT/S.p./GOx bioelectrode was 10.6 s with a detection limit of 73  $\mu\text{M}$  and average sensitivity of 9.79  $\mu\text{A mM}^{-1} \text{cm}^{-2}$ .

Despite the previously reported studies, whereas the amperometric responses of GOx-based electrodes registered during the oxidation of glucose were related to direct or quasi-direct electron transfer,<sup>27,28</sup> based on the results obtained herein, it can be concluded that the decrease of cathodic current cannot be entirely linked to the enzymatic catalytic current due to a few reasons: (i) it is seen that after the initial injection of 1 mM glucose, the obtained current response was higher than that initiated by the addition of similar or even three times more-concentrated substrate (Fig. 5a); (ii) if the oxygen was removed by N<sub>2</sub> bubbling, no significant changes in current were observed even after the addition of 12.5 mM glucose during the chronoamperometric measurements at the identical potential of  $-385$  mV. These results match those registered by CV analysis (Fig. 3a). Considering that the current starts to decrease from  $-25$  mV upon glucose addition, which is far away from the thermodynamic potential of the FAD/FADH<sub>2</sub> redox pair, the

obtained current responses can be related to changes in ORR rate. This reduction can be caused due to the consumption of O<sub>2</sub> by GOx (FAD) that use oxygen as a natural electron acceptor, thus being lower concentrations of dissolved O<sub>2</sub> accessible to the reduction on CNT-based electrode. Following this logical sequence, the amperometric responses of GC/PEI/CNT/S.p./GOx bioelectrode mostly can be related to the oxidation of glucose and the depletion of O<sub>2</sub>. By trying to find the application of this effect, it was observed that such an electrode design could be utilized for glucose monitoring; however, the detection range was determined to be between 1 and 3 mM of glucose (Fig. 5b, insets). Moreover, this interval can be extended if the buffer solution is exchanged after each chronoamperometric measurement. The registered calibration curve is characterized by significant linear regression between 250  $\mu\text{M}$  and 5 mM of glucose, which obeys the variation that can be well described using the equation of  $J$  ( $\mu\text{A cm}^{-2}$ ) =  $9.81 \cdot 10^{-6} \cdot C$  (mM) +  $6.62 \cdot 10^{-6}$  ( $R^2 = 0.977$ ). The average sensitivity of GC/PEI/CNT/S.p./GOx bioelectrode towards the addition of glucose is calculated to be 15.09  $\mu\text{A mM}^{-1} \text{cm}^{-2}$  with a response time of 14.5 s and a detection limit close to the value of 118  $\mu\text{M}$  (Fig. 5c, insets). These results allow us to predict that GC/PEI/CNT/S.p./GOx bioanode can be appropriate for glucose monitoring in aqueous solutions.

## Discussion

The two redox waves identified as FAD/FADH<sub>2</sub> redox pair at the potentials ranging from  $-480$  to  $-430$  mV vs Ag/AgCl (pH = 7) were considered truly evidence of GOx(FAD) immobilization on the nanostructured electrodes in the vast majority of reported papers. Furthermore, the drop in the reduction current occurring as a response caused by the addition of glucose was usually claimed as an unquestionable confirmation of DET between GOx(FAD) and various nanostructures, including carbon-based nanomaterials that can access the redox cofactor. Such explanation was commonly acceptable until the statement provided by Wilson, which has been defined that GOx cannot undergo DET.<sup>12</sup> It has been highlighted that H<sub>2</sub>O<sub>2</sub>, a product of the ORR and enzymatic reactions, can reduce itself on metal oxides-based NPs incorporated into conducting polymers<sup>38–41</sup> or CNT-based structures,<sup>10</sup> thus affecting the reduction current obtained from enzymatic electrodes. Assuming that CNT has  $\leq 2\%$  of metal oxide-based impurities (as it is in the case of this study), which exhibit extremely high catalytic activity towards H<sub>2</sub>O<sub>2</sub> reduction demonstrated above, it does not have a significant impact on GC/PEI/CNT/S.p./GOx bioelectrode current responses even in solutions containing 2 mM of H<sub>2</sub>O<sub>2</sub> (data not shown). This observation is most likely attributed to the low content of metal oxide-based residues surrounded by lots of carbon, thus isolating them from the electrode/solution interface. It has been hypothesized that this decrease in current is related to oxygen depletion because it serves as an electron acceptor during the enzymatic reaction.<sup>42</sup> Moreover, as highlighted above, CNT modified electrodes generated a similar response to glucose in air-saturated solutions. This phenomenon can be a critical component that affects and causes

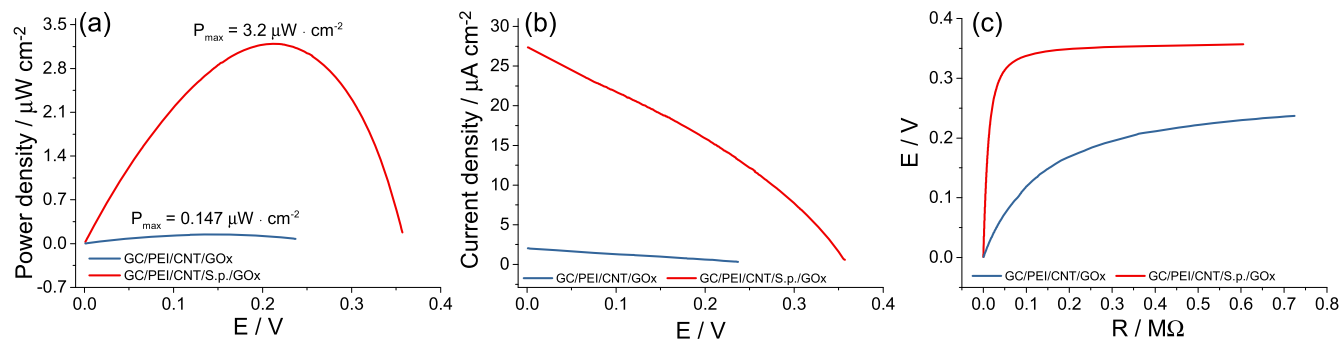


**Figure 4.** Comparison of GC/PEI/CNT/GOx and GC/PEI/CNT/S.p./GOx bioanodes' produced power (a) and current (b) density and their potential dependence on applied resistance (c) registered in air-saturated phosphate/acetate buffer solution (pH = 6) containing 12.5 mM of glucose.

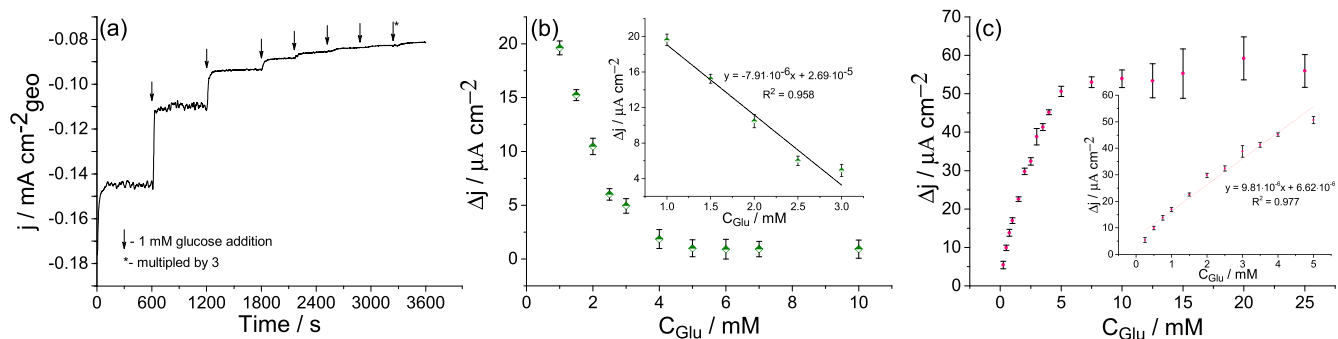


**Figure 5.** Chronoamperometric evaluation of GC/PEI/CNT/S.p./GOx bioelectrode (a) in air-saturated A-PBS at an applied potential of  $-385$  mV (vs Ag/AgCl) upon continuous addition of 1 mM of glucose. Calibration curves were registered in the same buffer solution (b) and replaced after glucose injection (c). *Insets:* the linear responses of GC/PEI/CNT/S.p./GOx bioelectrode towards the addition of glucose.

the cathodic current response to glucose. The origin of this phenomenon probably can be mainly prescribed to the physical process described above. These ideas are further justified by the control experiments with L-glucose that are presented below. As evidenced by control measurements, no significant changes in current were observed in the absence of ferrocene (Fig. 6e, curves 3, 4), thus confirming that catalytic activity of GOx does not occur without the assistance of redox mediators.<sup>43</sup> However, it was shown that GOx immobilized on CNT modified by *S. platensis*-based lysate remains its enzymatic activity towards glucose oxidation (Fig. 6e). Furthermore, it was observed that the catalytic current registered in the case with algae enriched bioelectrode was 10.4% higher (Fig. 6e, curve 1), thus specifying that *S. platensis*-based lysate probably can facilitate the immobilization of GOx and serve as a biological redox

mediator, ensuring the higher electron transfer rate. These results match well with those obtained via power density measurements, where the generated maximal power output was 14.4 times higher if the algae cell lysate was comprised in the bioelectrode design.

It is acceptable that the origin of two redox pairs registered during CV analysis at the potential window from  $-355$  to  $-455$  mV vs Ag/AgCl is based on the reduction/oxidation of the FAD/FADH<sub>2</sub> redox pair. However, some issues remain questionable: have these peaks appeared due to GOx(FAD) adsorption or free FAD that usually exists in the solution of GOx due to dissociation from the native enzyme structure. Considering that the GOx enzyme remains in its catalytic activity, as evidenced by control experiments with ferrocene, the origin of FAD/FADH<sub>2</sub> redox pairs is mostly related to free flavin being in the commercial enzyme aliquot. To clarify this

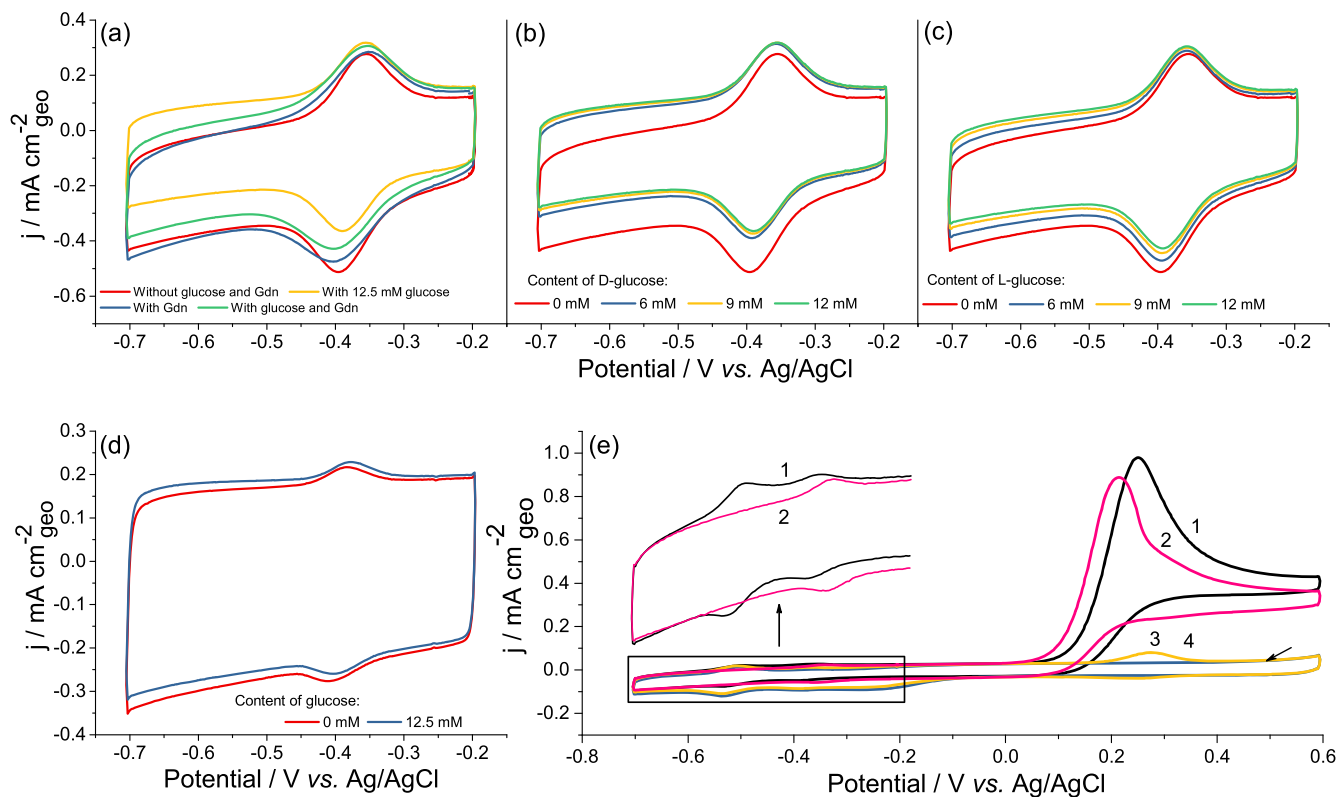


**Figure 6.** Cyclic voltammograms recorded in air-saturated phosphate/acetate buffer ( $\text{pH} = 6$ ) at a scan rate of  $40 \text{ mV s}^{-1}$  for GC/PEI/CNT/GOx electrode in various conditions: (a) before and after incubation in 3 M of guanidine hydrochloride solutions for 16 h; CV profiles obtained in the solutions containing different concentration of D-glucose (b) and L-glucose (c); CVs curves observed with GC/PEI/CNT electrode covered by 12 kDa dialysis membrane on which the exact content of GOx was drop-casted and immobilized following identical conditions is presented (d). In (e), the comparison of GC/PEI/CNT/S.p./GOx catalytic activity is represented (curve 1), and GC/PEI/CNT/GOx (curve 2) bioelectrodes evaluated in A-PBS solution containing 0.5 mM of ferrocene and 12.5 mM of glucose. Curves 3 and 4 are registered in the absence of glucose with and without ferrocene addition and correspond to the control measurements recorded at the scan rate of  $5 \text{ mV s}^{-1}$ .



assumption, a few control experiments were conducted with the assistance of guanidine hydrochloride (Fig. 6a), L-glucose (Figs. 6b and 6c) and dialysis membrane (Fig. 6d). It is commonly accepted that guanidine hydrochloride (usually at high concentrations) can easily strip the FAD from GOx or even denature GOx, removing it from the electrode surface.<sup>44</sup> Contrariwise it has no impact on removing free FAD adsorbed on the CNT surface.<sup>45</sup> As presented in Fig. 7a, after the incubation of GC/PEI/CNT/GOx bioelectrode in 3 M guanidine hydrochloride for 16 h, the FAD/FADH<sub>2</sub> redox peaks remained well-defined with minor changes in their  $E_{pc}$  value from -394 to -402 mV. Comparing their charge densities calculated by integration of cathodic peak current provided by electrode after storage in guanidine hydrochloride for 16 h was approximately 0.25  $\mu\text{C cm}^{-2}$  lower than that of not treated electrode. Surprisingly, the relative current response upon the addition of 12.5 mM glucose was approximately 3.2 times higher in the case when an electrode was not stored in the solution containing 3 M of guanidine hydrochloride, thus supplementing the hypothesis that some FAD adsorbed on CNT probably can be "in contact" with native enzyme as suggested in earlier studies.<sup>27</sup> On the other hand, it is contrary to GOx spatial structure and the distance between the redox-active centre and enzyme surface, limiting any direct redox communication with solid electrodes.<sup>43</sup> From this perspective, this phenomenon probably can arise due to the adsorption of some guanidine hydrochloride or FAD molecules on negatively charged carboxyl groups of CNT. These ideas are more speculative and need further investigation, but it is beyond the scope of this study. Nevertheless, the further control experiments conducted herein support more detailed information about the origin of these peaks, especially those with L-glucose and dialysis membranes. As presented in Figs. 7b and 7c, after a series addition of D-glucose and L-glucose, the current response is similar but not identical. Taking into account that the GOx enzyme catalyses the oxidation of D-glucose  $\beta$ -anomer approximately 150 times quicker than  $\alpha$ -anomer,<sup>46</sup> all glucose solutions used in this study were prepared 24 h before the experiment until the equilibrium between  $\alpha$  and  $\beta$  forms was established. Because L-glucose cannot be used as a substrate of GOx from *A. niger*,<sup>10</sup> the obtained current response after L-glucose addition (Fig. 6c) probably can be related to its adsorption on CNT or with changes due to variation in solution viscosity. It was concluded that both physical phenomena could decrease the ORR rate, leading to the reduced cathodic current response. This effect has usually been named a sign of DET; however, some exercises need to be solved with this interpretation. Regarding Bartlett's investigations, the results based on L-glucose complement each other, proving that the GOx enzyme adsorbed on CNT cannot undergo DET.<sup>10</sup> Lastly, the control test using a 12 kDa dialysis membrane was carried out to verify the presence of free FAD adsorbed on CNT after GOx immobilization. It is widely recognized that free flavin can penetrate through a membrane differently than GOx, whereas the molar mass varies from 150 to 180 kDa depending on the level of glycosylation.<sup>47</sup> Following this idea, the GC/PEI/CNT electrode was covered with a water-soaked dialysis membrane, rinsed carefully with DI water and dried in air. The prepared electrode was enriched by drop-casting 5  $\mu\text{l}$  of GOx and stored under the glutaraldehyde vapour overnight. The recorded CV profile contains the same pair of redox peaks that exhibit a similar response to glucose (Fig. 6d). It is evident that redox waves are smaller than those observed in Fig. 6b; however, this can be easily explained due to the reduced active CNT area available to FAD adsorption. Comparing the GC/PEI/GOx and GC/PEI/CNT/Membrane/GOx bioelectrodes prepared using fresh GOx solution (not older than two weeks), it can be assumed that FAD adsorption on CNT proceeded more effective because no reduction peaks were observed in the case with GC/PEI/GOx electrode (data not shown). Nevertheless, the results proved that free flavin exists in the solution of GOx in relatively high concentration, allowing us to speculate that the origin of FAD can be a consequence of the cofactor dissociation process occurring in the enzymatic solutions over time.<sup>46</sup>

## Conclusions

In summary, we developed and assessed the bioanode based on organelle containing *S. platensis* lysate, immobilized on the PEI and CNT modified glassy carbon electrode. The biological molecules conjugate enriched *S. platensis* lysate facilitate the immobilization of enzyme and act as a green (biological) redox mediator for GOx enzyme. The bioanode is relatively stable and can be operated in slightly acidic chloride-containing buffers (pH = 6). The designed bioanode exhibits the maximal OCP value of -259 mV vs Ag/AgCl (3 M KCl) in the presence of 12.5 mM of glucose. The maximum power output was 21.8 times higher and reached 3.2  $\mu\text{W cm}^{-2}$  if the algae cell lysate was used for bioanode design. These results indicate that *S. platensis*-based lysate might be suitable for developing biosensors and biofuel cells. Furthermore, it was shown that the influence of oxygen, hydrogen peroxide, CNT and metal oxides could affect the cathodic current, which is widely and incorrectly attributed to the "catalytic" current provided by bioelectrode towards the oxidation of glucose. It was assumed that the origin of reduction current decreases upon the addition of glucose as determined using cyclic voltammetry and chronoamperometry are mostly related not to direct charge transfer but to the depletion of oxygen in the electrolyte solutions.

## Acknowledgments

This research was funded by the European Social Fund under the No 09.3.3-LMT-K-712-19-0155 "Development of Competences of Scientists, other Researchers and Students through Practical Research Activities" measure.

## Author contribution statement

**Rokas Žalnėravičius:** Methodology, Validation, Conceptualization, Visualization, Writing - Original Draft, Writing - Review & Editing. **Arūnas Ramanavičius:** Resources, Supervision, Conceptualization, Writing - Review & Editing, Funding acquisition.

## ORCID

Rokas Žalnėravičius  <https://orcid.org/0000-0001-6571-5881>  
Arunas Ramanavicius  <https://orcid.org/0000-0002-0885-3556>

## References

1. United Nations, (2019), World Population Prospects: Highlights. ST/ESA/SER.A, 423-469, United Nations Reports Department of economic and social affairs, population division..
2. D. H. Lee, "Econometric assessment of bioenergy development." *Int. J. Hydrog. Energy*, **42**, 27701 (2017).
3. G. Joshi, J. K. Pandey, S. Rana, and D. S. Rawat, "Challenges and opportunities for the application of biofuel." *Renewable Sustainable Energy Rev*, **79**, 850 (2017).
4. C. Munoz-Cupa, Y. Hu, C. Xu (Charles), and A. Bassi, "An overview of microbial fuel cell usage in wastewater treatment, resource recovery and energy production." *Sci. Total Environ.*, **754**, 142429 (2021).
5. A. Singh, R. Sharma, D. Pant, and P. Malaviya, "Engineered algal biochar for contaminant remediation and electrochemical applications." *Sci. Total Environ.*, **774**, 145676 (2021).
6. S. Perazzoli, J. P. de Santana Neto, and H. Soares, "Prospects in bioelectrochemical technologies for wastewater treatment." *Water Sci. Technol.*, **78**, 1237 (2018).
7. D. Ratautas, A. Laurynėnas, M. Dagys, L. Marcinkevičienė, R. Meškys, and J. Kulyš, "High current, low redox potential mediatorless bioanode based on gold nanoparticles and glucose dehydrogenase from *Ewingella americana*." *Electrochim. Acta*, **199**, 254 (2016).
8. H. B. Gray and J. R. Winkler, "Electron tunneling through proteins." *Q. Rev. Biophys.*, **36**, 341 (2003).
9. C. C. Moser, J. M. Keske, K. Warncke, R. S. Farid, and P. L. Dutton, "Nature of biological electron transfer." *Nature*, **355**, 796 (1992).
10. P. N. Bartlett and F. A. Al-Lolage, "There is no evidence to support literature claims of direct electron transfer (DET) for native glucose oxidase (GOx) at carbon nanotubes or graphene." *J. Electroanal. Chem.*, **819**, 26 (2018).
11. A. Kausaitė, A. Ramanavičienė, and A. Ramanavičius, "Polyaniline synthesis catalysed by glucose oxidase." *Polymer*, **50**, 1846 (2009).
12. G. S. Wilson, "Native glucose oxidase does not undergo direct electron transfer." *Biosens. Bioelectron.*, **82**, vii (2016).

13. J. Zhang, J. Liu, H. Su, F. Sun, Z. Lu, and A. Su, "A wearable self-powered biosensor system integrated with diaper for detecting the urine glucose of diabetic patients." *Sens. Actuators B: Chem.*, **341**, 130046 (2021).
14. V. X. Le, H. Lee, N. S. Pham, S. Bong, H. Oh, S. H. Cho, and I. S. Shin, "Stainless steel 304 needle electrode for precise glucose biosensor with high signal-to-noise ratio." *Sens. Actuators B: Chem.*, **346**, 130552 (2021).
15. R. A. Soni, K. Sudhakar, and R. S. Rana, "Spirulina—from growth to nutritional product: a review." *Trends Food Sci. Technol.*, **69**, 157 (2017).
16. C. C. Fu, C. H. Su, T. C. Hung, C. H. Hsieh, D. Suryani, and W. T. Wu, "Effects of biomass weight and light intensity on the performance of photosynthetic microbial fuel cells with *Spirulina platensis*." *Bioresour. Technol.*, **18**, 4183 (2009).
17. C. C. Lin, C. H. Wei, C. I. Chen, C. J. Shieh, and Y. C. Liu, "Characteristics of the photosynthesis microbial fuel cell with a *Spirulina platensis* biofilm." *Bioresour. Technol.*, **135**, 640 (2013).
18. N. Longtin, D. Oliveira, A. Mahadevan, V. Gejji, C. Gomes, and S. Fernando, "Analysis of *Spirulina platensis* microalgal fuel cell." *J. Power Sources*, **486**, 229290 (2021).
19. Z. Yang, H. Pei, Q. Hou, L. Jiang, L. Zhang, and C. Nie, "Algal biofilm-assisted microbial fuel cell to enhance domestic wastewater treatment: nutrient, organics removal and bioenergy production." *Chem. Eng. J.*, **332**, 277 (2018).
20. M. M. Bradford, "A rapid and sensitive method for the quantitation of microgram quantities of protein utilizing the principle of protein-dye binding." *Anal. Biochem.*, **72**, 248 (1976).
21. Y. Weizmann, D. M. Chenoweth, and T. M. Swager, "Addressable terminally linked DNA-CNT nanowires." *J. Am. Chem. Soc.*, **132**, 14009 (2010).
22. N. Sezer and M. Koc, "Oxidative acid treatment of carbon nanotubes." *Surf. Interfaces*, **14**, 1 (2019).
23. A. Ramanavicius, A. Kausaite-Minkstimiene, I. Morkvenaite-Vilkonciene, P. Genys, R. Mikhailova, T. Semashko, J. Voronovic, and A. Ramanaviciene, "Biofuel cell based on glucose oxidase from *Penicillium funiculosum* 46.1 and horseradish peroxidase." *Chem. Eng. J.*, **264**, 165 (2015).
24. S. B. Bankar, M. V. Bule, R. S. Singhal, and L. Ananthanarayan, "Glucose oxidase—an overview." *Biotechnol. Adv.*, **27**, 489 (2009).
25. T. Ruzgas, "Enzyme-based (bio)fuel cells—bilirubin oxidase use." *Encyclopedia of Interfacial Chemistry: Surface Science and Electrochemistry* (Elsevier, Amsterdam, Netherlands) p.209 (2018).
26. S. Cosnier, M. Holzinger, and A. L. Goff, "Recent advances in carbon nanotube-based enzymatic fuel cells." *Front. Bioeng. Biotechnol.*, **2**, 45 (2014).
27. K. Hyun, S. W. Han, W. G. Koh, and Y. Kwon, "Direct electrochemistry of glucose oxidase immobilized on carbon nanotube for improving glucose sensing, Int. J. Hydrog." *Energy*, **40**, 2199 (2015).
28. Y. Liu, J. Zhang, Y. Cheng, and S. P. Jiang, "Effect of carbon nanotubes on direct electron transfer and electrocatalytic activity of immobilized glucose oxidase." *ACS omega*, **3**, 667 (2018).
29. Y. Wang, J. Li, and Z. Wei, "Transition-metal-oxide-based catalysts for the oxygen reduction reaction." *J. Mater. Chem. A*, **6**, 8194 (2018).
30. K. Jiang et al., "Highly selective oxygen reduction to hydrogen peroxide on transition metal single atom coordination." *Nat. Commun.*, **10**, 3997 (2019).
31. J. H. T. Luong, J. D. Glennon, A. Gedanken, and S. K. Vashist, "Achievement and assessment of direct electron transfer of glucose oxidase in electrochemical biosensing using carbon nanotubes, graphene, and their nanocomposites." *Microchim. Acta*, **184**, 369 (2017).
32. J. C. Byers, A. G. Güell, and P. R. Unwin, "Nanoscale electrocatalysis: visualizing oxygen reduction at pristine, kinked, and oxidized sites on individual carbon nanotubes." *J. Am. Chem. Soc.*, **136**, 11252 (2014).
33. E. Laviron, "General expression of the linear potential sweep voltammogram in the case of diffusionless electrochemical systems." *J. Electroanal. Chem.*, **101**, 19 (1979).
34. S. Palanisamy, R. Devasenathipathy, S. M. Chen, M. A. Ali, C. Karupiah, V. Balakumar, P. Prakash, M. S. Elshikh, and F. M. A. Al-Hemaid, "Direct electrochemistry of glucose oxidase at reduced graphene oxide and  $\beta$ -cyclodextrin composite modified electrode and application for glucose biosensing." *Electroanalysis*, **27**, 2412 (2015).
35. N. B. Duong, V. M. Truong, Y. S. Li, C. L. Wang, and H. Yang, "Improving the immobilization of glucose oxidase on carbon cloth via a hybrid approach of cross-linked chitosan/TPP matrices with Na polymers for high-performance self-pumping enzyme-based biofuel cells." *Energy Fuels*, **34**, 10050 (2020).
36. C. C. Fu, T. C. Hung, W. T. Wu, T. C. Wen, and C. H. Su, "Current and voltage responses in instant photosynthetic microbial cells with *Spirulina platensis*." *Biochem. Eng. J.*, **52**, 175 (2010).
37. S. Sevdá, V. K. Garlapati, S. Sharma, S. Bhattacharya, S. Mishra, T. R. Sreerishnan, and D. Pant, "Microalgae at niches of bioelectrochemical systems: a new platform for sustainable energy production coupled industrial effluent treatment." *Bioresour. Technol.*, **7**, 100290 (2019).
38. A. Ramanaviciene, G. Nastajute, V. Snitka, A. Kausaite, N. German, D. Barauskas-Memenas, and A. Ramanavicius, "Spectrophotometric evaluation of gold nanoparticles as red-ox mediator for glucose oxidase." *Sensor Actuat B-Chem.*, **137**, 483 (2009).
39. S. Ramanavicius and A. Ramanavicius, "Charge transfer and biocompatibility aspects in conducting polymers based enzymatic biosensors and biofuel cells." *Nanomaterials*, **11**, 371 (2021).
40. N. German, A. Ramanaviciene, and A. Ramanavicius, "Electrochemical deposition of gold nanoparticles on graphite rod for glucose biosensing." *Sensor Actuat B-Chem.*, **203**, 25 (2014).
41. N. German, A. Ramanavicius, and A. Ramanaviciene, "Amperometric glucose biosensor based on electrochemically deposited gold nanoparticles covered by polypyrrole." *Electroanalysis*, **29**, 1267 (2017).
42. M. Wooten, S. Karra, M. Zhang, and W. Gorski, "On the direct electron transfer, sensing, and enzyme activity in the glucose oxidase/carbon nanotubes system." *Anal. Chem.*, **86**, 752 (2014).
43. P. Bollella and E. Katz, "Enzyme-based biosensors: tackling electron transfer issues." *Sensors (Basel)*, **12**, 3517 (2020).
44. F. Scheller, G. Strand, B. Neumann, M. Kühn, and W. Ostrowski, "Polarographic reduction of the prosthetic in favoproteins." *Bioelectrochem. Bioenerg.*, **6**, 117 (1979).
45. R. M. Ianniello, T. J. Lindsay, and A. M. Yacynych, "Differential pulse voltammetric study of direct electron transfer in glucose oxidase chemically modified graphite electrodes." *Anal. Chem.*, **54**, 1098 (1982).
46. R. E. Holt and T. M. Cotton, "Free flavin interference in surface enhanced resonance Raman spectroscopy of glucose oxidase." *J. Am. Chem. Soc.*, **109**, 1841 (1987).
47. F. Belyad, A. A. Karkhanei, and J. Raheb, "Expression, characterization and one step purification of heterologous glucose oxidase gene from *Aspergillus niger* ATCC 9029 in *Pichia pastoris*." *EuPA Open Proteom.*, **19**, 1 (2018).